Modulation of localized solutions in a system of two coupled nonlinear Schrödinger equations

W. B. Cardoso,[1] A. T. Avelar,[1] and D. Bazeia[2]

[1]*Instituto de Física, Universidade Federal de Goiás, 74.001-970, Goiânia, Goiás, Brazil*

[2]*Departamento de Física, Universidade Federal da Paraíba, 58.051-970, João Pessoa, Paraíba, Brazil*

(Received 20 March 2012; revised manuscript received 4 July 2012; published 23 August 2012)

In this work we study localized solutions of a system of two coupled nonlinear Schrödinger equations, with the linear (potential) and nonlinear coefficients engendering spatial and temporal dependencies. Similarity transformations are used to convert the nonautonomous coupled equations into autonomous ones and we use the trial orbit method to help us solving them, presenting solutions in a general way. Numerical experiments are then used to verify the stability of the localized solutions.

DOI: 10.1103/PhysRevE.86.027601 PACS number(s): 05.45.Yv, 03.75.Lm

I. INTRODUCTION

Vector solitons are essential to the understanding of a diversity of physical systems that appear, for instance, in nonlinear optics [1], multispecies condensates [2], superchemistry [3], and plasma [4]. From the theoretical point of view, they present a richer propagation dynamics than scalar solitons due to the presence of cross-phase modulation leading to possible intensity redistributions between the components in collision events [5]. For applications, the collision dynamics of vector solitons can be employed to implement all-optical digital computation without radiative losses [6] and information transfer [7].

In the investigation of vector solitons from a system of coupled nonlinear Schrödinger equations (CNLSEs), the so-called Manakov model [1] has received a great deal of attention. In this scenario, experimental observations of temporal vector soliton propagation and collisions in a linearly birefringent optical fiber [8] and spatial vector solitons in AlGaAs [9] and photorefractive crystals [10] have been reported. In the case of Bose-Einstein condensates (BECs), two-component condensates have been realized in rubidium atoms in a magnetic trap [2] and in sodium atoms in an optical trap [11].

Although most of the above-mentioned previous studies make use of autonomous CNLSEs, there are more general situations well described by nonautonomous CNLSEs where the potentials and nonlinearities are modulated in space and time [12]. Focusing on this, in this work we study localized solutions of one-dimensional CNLSEs with spatial and temporal dependencies on the linear (potential) and nonlinear coefficients. To search for different vector solitons of nonautonomous CNLSEs, we employ the following strategy. First, a similarity transformation technique [13–17] is used to transform nonautonomous CNLSEs into autonomous CNLSEs. The latter can then be decoupled by applying the trial orbit method [18], which involves choosing specific orbits connecting the minima of the field potential associated with autonomous CNLSEs. Finally, the decoupled equations are solved by the first-order formalism for lumps [19,20]. As we show, this strategy leads to several solutions of nonautonomous CNLSEs, which we can see as a gain in terms of a systematic way of solving autonomous CNLSEs.

II. THEORETICAL MODEL

We consider an autonomous CNLSE, which can be written as

$$i\partial_t\psi_j = -\tfrac{1}{2}\partial_x^2\psi_j + V_j\psi_j + (g_{jj}|\psi_j|^2 + g_{jk}|\psi_k|^2)\psi_j, \quad (1)$$

with $j \neq k = \{1,2\}$; $\psi_1 \equiv \psi(x,t)$; $\psi_2 \equiv \phi(x,t)$; $\partial_t \equiv \partial/\partial t$, $\partial_x^2 \equiv \partial^2/\partial x^2$, etc.; and $V_j = V_j(x,t)$. These equations can be used to describe the density profile of a BEC with two components (two species of atoms, say) in which nonlinearities are controlled by using Feschbach resonances or pulse propagation along two orthogonal polarization axes in inhomogeneous nonlinear optical fibers in which the linear part of the refractive index depends on the spatial position [21].

To start our strategy of finding specific solutions we use the ansatz

$$\psi_j(x,t) = \rho(t)e^{i\eta(x,t)}\Psi_j[\zeta(x,t),\tau(t)] \quad (2)$$

to connect the solution of the coupled equations (1) with those of the autonomous system given by

$$i\partial_\tau\Psi_j = -\tfrac{1}{2}\partial_\zeta^2\Psi_j + (G_{jj}|\Psi_j|^2 + G_{jk}|\Psi_k|^2)\Psi_j, \quad (3)$$

with $j \neq k$ and G_{jk} (and G_{jj}) now being constant coefficients. To get this we must have

$$\zeta_{xx} = 0, \quad \tau_t = \zeta_x^2, \quad (4)$$

$$\zeta_t + \zeta_x\eta_x = 0, \quad \rho_t + \tfrac{1}{2}\rho\eta_{xx} = 0, \quad (5)$$

$$V_i = -\frac{1}{2}\eta_x^2 - \eta_t, \quad g_{ij} = \frac{G_{i,j}\zeta_x^2}{\rho^2}. \quad (6)$$

Thus, using the similarity transformations (2), we could change the nonautonomous system (1) into an autonomous one, described by Eq. (3), with the set of equations (4)–(6) being satisfied to validate the procedure.

From Eq. (4) we obtain $\zeta(x,t) = \gamma(t)x + \delta(t)$ and $\tau(t) = \int \gamma^2 dt$, which when substituted into Eq. (5) results in

$$\eta(x,t) = -\frac{\gamma_t}{2\gamma}x^2 - \frac{\delta_t}{\gamma}x + \beta(t), \quad \rho(t) = \sqrt{\gamma}, \quad (7)$$

where we have omitted the constant of integration of the preceding equation, for simplicity. We can rewrite the nonlinearities and potentials in Eq. (6) as $g_{jk}(t) = G_{jk}\gamma(t)$ and

$$V_j(x,t) = \left(\frac{\gamma_{tt}}{2\gamma} - \frac{\gamma_t^2}{\gamma^2}\right)x^2 + \left(\frac{\delta_{tt}}{\gamma} - \frac{2\gamma_t\delta_t}{\gamma^2}\right)x - \left(\frac{\delta_t^2}{2\gamma^2} + \beta_t\right).$$

In the case of BECs, these potentials and nonlinearities are experimentally feasible using external magnetic and optical pulses and the Feshbach resonance.

III. SPECIFIC SOLUTIONS

If we consider solutions of the form $\Psi_1(\zeta,\tau) = A(\zeta)e^{-i\mu\tau}$ and $\Psi_2(\zeta,\tau) = B(\zeta)e^{-i\nu\tau}$ in Eq. (3) we obtain

$$\mu A = -\tfrac{1}{2}A_{\zeta\zeta} + (G_{11}A^2 + G_{12}B^2)A, \tag{8}$$

$$\nu B = -\tfrac{1}{2}B_{\zeta\zeta} + (G_{21}A^2 + G_{22}B^2)B. \tag{9}$$

To find analytical solutions for Eqs. (8) and (9) we use the trial orbit method to decouple these equations. Following Ref. [18], we can construct a field potential $\mathfrak{V}(A,B)$ such that $A_{\zeta\zeta} = \partial\mathfrak{V}/\partial A$ and $B_{\zeta\zeta} = \partial\mathfrak{V}/\partial B$ and choose a specific orbit condition $g(A,B) = 0$ having the free parameter adjusted to be compatible with the field potential. In our case, the condition $G_{12} = G_{21}$ is required to construct the field potential associated with Eqs. (8) and (9). In this field potential we will see that the minimum {0,0} is linked with the existence of localized solutions while the four minima $\{\pm[(\mu G_{22} - G_{12}\nu)/(G_{11}G_{22} - G_{12}^2)]^{1/2}, \operatorname{sgn}(G22)[(\nu G_{11} - G_{12}\mu)/(G_{11}G_{22} - G_{12}^2)]^{1/2}\}$ and $\{\pm[(\mu G_{22} - G_{12}\nu)/(G_{11}G_{22} - G_{12}^2)]^{1/2}, -\operatorname{sgn}(G22)[(\nu G_{11} - G_{12}\mu)/(G_{11}G_{22} - G_{12}^2)]^{1/2}\}$ are linked with delocalized solutions. Choosing the orbit condition $A = \alpha B$ (which presents a similar profile but with different amplitude), we decouple the system (8) and (9) into two decoupled equations presenting cubic nonlinearities as

$$\mu A = -\tfrac{1}{2}A_{\zeta\zeta} + (G_{11} + G_{12}/\alpha^2)A^3, \tag{10}$$

$$\nu B = -\tfrac{1}{2}B_{\zeta\zeta} + (G_{22} + \alpha^2 G_{21})B^3. \tag{11}$$

In the following sections we show two examples: bright-bright and dark-dark solitons. In these examples we use $\gamma = [2 - \cos^2(\omega t)]^{-1}$ and $\delta = 0$ (with $\beta_t = -\delta_t^2/2\gamma^2$ in all cases). In this way we get

$$\tau(t) = \frac{3}{8\omega}\sqrt{2}\arctan[\sqrt{2}\tan(\omega t)] + \frac{1}{4\omega}\tan(\omega t)/[2\tan^2(\omega t) + 1]$$

and $\zeta(x,t) = x/[2 - \cos^2(\omega t)]$. This will lead us to

$$\rho(t) = [2 - \cos^2(\omega t)]^{-1/2}, \tag{12}$$

$$\eta(x,t) = \frac{\cos(\omega t)\sin(\omega t)}{2 - \cos^2(\omega t)}\omega x^2, \tag{13}$$

$$V(x,t) = \frac{[2\cos^2(\omega t) - 1]}{\cos^2(\omega t) - 2}\omega^2 x^2. \tag{14}$$

Figure 1 shows the linear coefficient (potential) of the CNLSE [Eq. (1)] given by Eq. (14) versus the spatial and temporal coordinates. Note that the potential is quadratic in spatial coordinates and oscillates due to its temporal dependence.

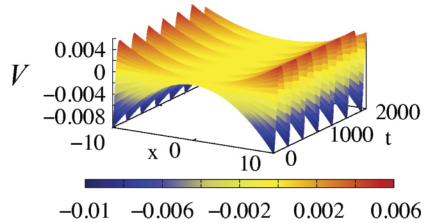

FIG. 1. (Color online) Linear coefficient (potential) of the CNLSEs given by Eq. (14) with $\omega = 0.01$.

A. Bright-bright solitons

The minimum of the field potential {0,0} is attained taking the conditions $\mu,\nu < 0$. Inserting the field potential $\mathfrak{V}$ in the orbit condition (see Ref. [18] for more details) we obtain specific relations for the parameters such that for the orbit $A = \alpha B$ we get $\nu = \mu$ and $G_{11} = (G_{12}(\alpha^2 - 1) + G_{22})/\alpha^2$. At this point we have four parameters to be determined in adjustment with the solutions of Eqs. (10) and (11).

As an example let us consider the solution $A(\zeta) = \Lambda\,\mathrm{sech}(\lambda\zeta)$, with $\lambda = \sqrt{-2\mu}$ and $\Lambda = [2\mu/(G_{12}\alpha^2 + G_{22})]^{1/2}$. The total power $P = \int_{-\infty}^{\infty}(|A|^2 + |B|^2)d\zeta$ of the autonomous coupled equation is given by $P = -2\sqrt{-2\mu}(1 + \alpha^2)/(G_{12}\alpha^2 + G_{22})$. Since the evolutions of A and B are governed by a single parameter (μ in this case), an approach similar to the Vakhitov-Kolokolov criterion for the stability is usually for the total power, i.e., stable solutions are obtained since $dP/d\mu = \sqrt{2}(1 + \alpha^2)/[\sqrt{-\mu}(G_{12}\alpha^2 + G_{22})] > 0$ [22]. Localized solutions of Eqs. (10) and (11) require negative cubic coefficients, such that $G_{22} + \alpha^2 G_{12} < 0$, that satisfy $dP/d\mu > 0$ for any $\mu < 0$, i.e., stable solutions.

Considering $P = 2$, for simplicity, we get $G_{22} = -\sqrt{-2\mu}(1 + \alpha^2) - G_{12}\alpha^2$. To give an explicit example we have chosen $\mu = -0.5$, $\alpha = \sqrt{2}$, and $G_{12} = -1$. The G_{11} and G_{22} are obtained by the above conditions.

Considering the above example, we can write the complete solutions in the form

$$\psi_j(x,t) = \frac{\sqrt{6/j}}{3}\frac{\exp\left(\frac{i\omega x^2\cos(\omega t)\sin(\omega t)}{2-\cos^2(\omega t)}\right)}{\sqrt{2 - \cos^2(\omega t)}}\mathrm{sech}\left(\frac{x}{\cos^2(\omega t) - 2}\right). \tag{15}$$

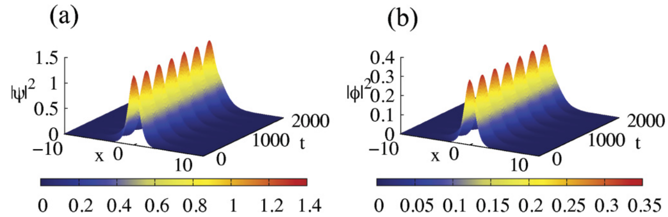

FIG. 2. (Color online) Plots of (a) $|\psi|^2$ and (b) $|\phi|^2$, corresponding to Eq. (15) with $j = 1,2$, respectively. Here we have used the modulation frequency $\omega = 0.01$.

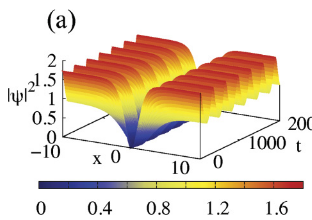

FIG. 3. (Color online) Plots of (a) $|\psi|^2$ and (b) $|\phi|^2$, corresponding to Eqs. (16) and (17), respectively, with modulation frequency $\omega = 0.01$.

In Figs. 2(a) and 2(b) we display the solutions given by Eq. (15) for $j = 1,2$, respectively. Note that both solutions show a breathing pattern due to the external modulation of the static solutions.

B. Dark-dark solitons

In this example we look for solutions that connect two minima of the field potential. The requirements for the minima of the potential are $\mathrm{sgn}\{G_{11}/(G_{11}G_{22} - G_{12}^2)\}(G_{12}\nu - \mu G_{22}) < 0$ and $\mathrm{sgn}\{G_{22}/(G_{11}G_{22} - G_{12}^2)\}(G_{11}\nu - G_{12}\mu) > 0$ (sgn is the signal function). Via the orbit condition for the minima we take $\alpha = \sqrt{(\mu G_{22} - G_{12}\nu)/(G_{11}\nu - G_{12}\mu)}$, which associates the relative amplitude of the fields with the value of the external parameters. As a result, we get $\nu = \mu$ assuming $G_{12}^2 \neq G_{11}G_{22}$ and $G_{22} \neq G_{12}$ (to avoid divergence analysis), which simplify the analysis based on a single evolution parameter. For positive nonlinear parameters (a requirement for delocalized solutions) we will assume $(G_{11}G_{22} - G_{12}^2)/(G_{11} - G_{12}) > 0$ and $(G_{11}G_{22} - G_{12}^2)/(G_{22} - G_{12}) > 0$.

At this point we look for solutions given by $A(\zeta) = \Lambda \tanh(\lambda\zeta)$, where $\Lambda = \lambda\sqrt{(G_{11} - G_{12})/(G_{11}G_{22} - G_{12}^2)}$ and $\lambda = \sqrt{\mu}$. It is clear that the total power is an infinity quantity. So by use of the renormalized total power [21] we obtain $P = 2\sqrt{\mu}(2G_{12} - G_{11} - G_{22})/(G_{12}^2 - G_{11}G_{22})$. We will focus on parameter values such that $dP/d\mu > 0$, i.e., $\mathrm{sgn}\{2G_{12} - G_{11} - G_{22}\} = \mathrm{sgn}\{G_{12}^2 - G_{11}G_{22}\}$. It is worth stressing that $dP/d\mu > 0$ is not usually a criterion for dark solitons (see Ref. [21] for more details). Here this choice only gives a direction for our numerical tests.

As we have done previously, taking $P = 2$ for simplicity we get $G_{11} = (-2\sqrt{\mu}G_{12} + \sqrt{\mu}G_{22} + G_{12}^2)/(G_{22} - \sqrt{\mu})$. To give an explicit example we have chosen $\mu = 0.5$, $G_{12} = 0.25$, and $G_{22} = 1$. In this case we will have

$$\psi(x,t) = -\left(\frac{\sqrt{2}(2-\sqrt{2})}{3}\right)^{1/2} \frac{\exp\left(\frac{i\omega x^2 \cos(\omega t)\sin(\omega t)}{2-\cos^2(\omega t)}\right)}{\sqrt{2-\cos^2(\omega t)}} \times \tanh\left(\frac{x}{\sqrt{2}[\cos^2(\omega t) - 2]}\right), \tag{16}$$

$$\phi(x,t) = -\left(\frac{2\sqrt{2}-1}{3\sqrt{2}}\right)^{1/2} \frac{\exp\left(\frac{i\omega x^2 \cos(\omega t)\sin(\omega t)}{2-\cos^2(\omega t)}\right)}{\sqrt{2-\cos^2(\omega t)}} \times \tanh\left(\frac{x}{\sqrt{2}[\cos^2(\omega t) - 2]}\right). \tag{17}$$

Figures 3(a) and 3(b) display the solutions (16) and (17), respectively. Note that, similar to the bright-bright case, both solutions show a breathing pattern with frequency ω due to the external modulation associated with the choice of the $\gamma(t)$. Also note that the motion of the center of mass can be controlled by the $\delta(t)$ function. These choices depend on experimental parameters associated with the external parameters such as magnetic and optical fields, lead by the Feshbach resonance management.

C. Bright-dark solitons

Let us now investigate another pair of solutions of the system given by Eq. (1). Here we use the orbit $|\Psi|^2 = \alpha\left(1 - |\Phi|^2\right)$, from with we can decouple the system (3) as follows:

$$(\mu - G_{12})A = -\tfrac{1}{2}A_{\zeta\zeta} + (G_{11} - G_{12}/\alpha)A^3, \tag{18}$$

$$(\nu - \alpha G_{12})B = -\tfrac{1}{2}B_{\zeta\zeta} + (G_{22} - \alpha G_{12})B^3, \tag{19}$$

where we have employed the stationary configurations given by Eqs. (20) and (21). In this case we will have a localized solution in one field plus a delocalized solution in the other. Thus we require that the minima of the field potential are given by $\{0, \pm 1\}$ since the orbit condition for the minima results in $G_{22} = \nu$, with necessary conditions $\nu > 0$ and $\mu < G_{12}$. We obtain $G_{12} = (2\mu + \nu)/(\alpha + 2)$ and $G_{11} = (2\mu\alpha + 2\mu - \nu)/[\alpha(\alpha + 2)]$, reducing the number of free parameters that describes the solution.

Next we use the formal solution $B(x) = \tanh(\Lambda\zeta)$, where $\Lambda = \sqrt{-2(\mu\alpha - \nu)/(\alpha + 2)}$. We also use the same $\gamma(t)$, $\delta(t)$, and $\beta(t)$, maintaining the conditions (12)–(14) with the same form. We use the natural choices of the nonlinear parameters, i.e., a negative value for the localized solution and a positive value for the delocalized one. So we will have $\nu > 2\mu(\alpha + 1)$ and $\nu > \alpha(2\mu + \nu)/(\alpha + 2)$ (assuming $\alpha > 0$). The complete solution can be written in the form

$$\psi(x,t) = \sqrt{\frac{2}{2-\cos^2(\omega t)}}\exp\left(\frac{i\omega x^2\cos(\omega t)\sin(\omega t)}{\cos^2(\omega t) - 2}\right) \times \mathrm{sech}\left(\sqrt{\frac{3}{2}}\frac{x}{\cos^2(\omega t) - 2}\right), \tag{20}$$

$$\phi(x,t) = -\frac{1}{\sqrt{2-\cos^2(\omega t)}}\exp\left(\frac{i\omega x^2\cos(\omega t)\sin(\omega t)}{\cos^2(\omega t) - 2}\right) \times \tanh\left(\sqrt{\frac{3}{2}}\frac{x}{\cos^2(\omega t) - 2}\right), \tag{21}$$

where we have used $\alpha = 2$ and $\mu = -\nu = 1$.

In Fig. 4 we show the profile of $|\psi|^2$ and $|\phi|^2$. Since both fields (particle densities in the case of BECs) experience

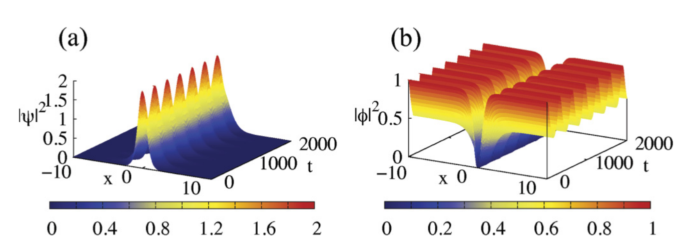

FIG. 4. (Color online) Plots of (a) $|\psi|^2$ and (b) $|\phi|^2$, corresponding to Eqs. (20) and (21), respectively, with modulation frequency $\omega = 0.01$.

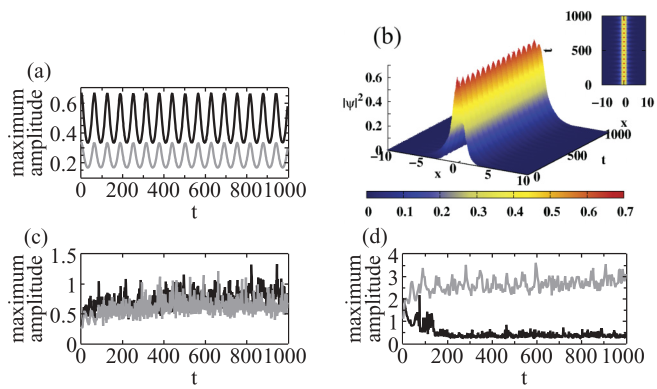

FIG. 5. (Color online) Analysis of stability. The maximum amplitudes of $|\psi|^2$ and $|\phi|^2$ are shown as black and gray lines, respectively. In this sense, we show in (a), (c), and (d) the maximum amplitudes for cases 1, 2, and 3, respectively. The profile of $|\psi|^2$ for case 1 is shown in (b). Similar behaviors are obtained for $|\phi|^2$. Here we consider the evolution up to $t = 1000$, but the same behavior was observed up to $t = 10\,000$, which is not shown here due to problems in the resolution of the figures because of the number of oscillations.

the same linear coefficient (potential) with similar nonlinear coefficients, the periods of oscillations are equal. This fact is feasible in the case of BECs since the external fields can be perceived in a similar way for the two components. Note the two distinct behaviors, one localized and the other delocalized. Experimentally, this behavior is similar to the BECs of ^{87}Rb [2] and ^{7}Li [11] atoms.

To verify the stability of the solutions presented above, we have employed numerical simulations based on split-step Crank-Nicholson algorithms, working with finite-difference methods. For a detailed description of these algorithms and FORTRAN programs for the time-dependent Gross-Pitaevskii equation, see Ref. [23]. We have used the time step $\Delta t = 10^{-4}$ and the space step $\Delta x = 10^{-2}$ for a good convergence [23]. First we consider the analytical solution of each example above in the time $t = 0$. Then the input of the program is given by this solution with a random perturbation (with 5% of the amplitude) of a uniform distribution with its mean centered at zero. Next this profile is lead to evolve up to $t = 10\,000$, which corresponds to a real time of $\sim 10s$, which is greater than the lifetime of the BEC (~ 3 s) since the dimensionless time is proportional to ω_z^{-1}, with $\omega_z \sim 1$–10^3 Hz being the axial oscillation frequency (see Ref. [11]). Note that the effective modulation frequency given by $\omega \times \omega_z$ leads to the period of oscillation of the potential [Eq. (14)] equal to $\pi/(\omega \times \omega_z)$. A stable coupled solution is verified for the first example [Eq. (15)]. However, the last two cases have presented an unstable behavior under the considered perturbations. Figure 5 displays the time evolution of the maximum values of $|\psi|^2$ and $|\phi|^2$ as black and gray lines, respectively. In Fig. 5(b) we display the profile $|\psi|^2$ of Eq. (15). It is worth mentioning that the stability of the solutions is a necessary condition for them to be experimentally feasible. Thus the latter two solutions are treated in this study as examples of the application of the method.

IV. CONCLUSION

In this work we investigated the presence of solutions for a system of two CNLSEs. As a result we have shown that inhomogeneous CNLSEs can present stable solutions for both field components. This was done through the use of the similarity transformation method [14] plus the trial orbit method [18]. We found explicit analytical solutions in the case $|\Phi|^2 = \alpha^2|\Psi|^2$ for two distinct sets of parameters. We also found analytical solutions for $|\Phi|^2 = \alpha(1 - |\Psi|^2)$ for a given set of parameters. The first set of solutions seems to be stable, while the two other sets appear to be unstable under small perturbations in their corresponding amplitudes.

ACKNOWLEDGMENTS

We thank the Brazilian agencies Conselho Nacional de Desenvolvimento Científico e Tecnológico and Instituto Nacional de Ciência e Tecnologia de Informação Quântica for partial financial support.

[1] S. V. Manakov, Zh. Eksp. Teor. Fiz. **65**, 505 (1973) [Sov. Phys. JETP **38**, 248 (1974)].
[2] C. J. Myatt, E. A. Burt, R. W. Ghrist, E. A. Cornell, and C. E. Wieman, Phys. Rev. Lett. **78**, 586 (1997); J. Babarro, M. J. Paz-Alonso, H. Michinel, J. R. Salgueiro, and D. N. Olivieri, Phys. Rev. A **71**, 043608 (2005).
[3] P. D. Drummond, K. V. Kheruntsyan, and H. He, Phys. Rev. Lett. **81**, 3055 (1998).
[4] E. Infeld and G. Rowlands, *Nonlinear Waves, Solitons, and Chaos*, 2nd ed. (Cambridge University Press, Cambridge, 2000).
[5] R. Radhakrishnan, M. Lakshmanan, and J. Hietarinta, Phys. Rev. E **56**, 2213 (1997); R. Radhakrishnan, P. T. Dinda, and G. Millot, *ibid*. **69**, 046607 (2004).
[6] M. H. Jakubowski, K. Steiglitz, and R. Squier, Phys. Rev. E **58**, 6752 (1998).
[7] C. Anastassiou *et al*., Opt. Lett. **26**, 1498 (2001).
[8] D. Rand *et al*., Phys. Rev. Lett. **98**, 053902 (2007).
[9] J. U. Kang, G. I. Stegeman, J. S. Aitchison, and N. Akhmediev, Phys. Rev. Lett. **76**, 3699 (1996).
[10] Z. Chen *et al*., J. Opt. Soc. Am. B **14**, 3066 (1997).
[11] D. M. Stamper-Kurn *et al*., Phys. Rev. Lett. **80**, 2027 (1998).
[12] W. B. Cardoso *et al*., Phys. Lett. A **374**, 2356 (2010).
[13] W. B. Cardoso, A. T. Avelar, and D. Bazeia, Phys. Rev. E **83**, 036604 (2011).
[14] J. Belmonte-Beitia, V. M. Pérez-García, V. Vekslerchik, and V. V. Konotop, Phys. Rev. Lett. **100**, 164102 (2008); A. T. Avelar, D. Bazeia, and W. B. Cardoso, Phys. Rev. E **79**, 025602(R) (2009).
[15] W. B. Cardoso, A. T. Avelar, and D. Bazeia, Nonlin. Anal. RWA **11**, 4269 (2010).

[16] A. T. Avelar, D. Bazeia, and W. B. Cardoso, Phys. Rev. E **82**, 057601 (2010).
[17] W. B. Cardoso, A. T. Avelar, and D. Bazeia, Phys. Lett. A **374**, 2640 (2010).
[18] R. Rajaraman, Phys. Rev. Lett. **42**, 200 (1979); D. Bazeia *et al.*, Mod. Phys. Lett. A **17**, 1945 (2002).
[19] A. T. Avelar *et al.*, Eur. Phys. J. C **55**, 133 (2008).
[20] A. T. Avelar *et al.*, Phys. Lett. A **374**, 222 (2009).
[21] Y. S. Kivshar and G. P. Agrawal, *Optical Solitons: From Fibers to Photonic Crystals* (Academic, San Diego, 2003).
[22] Y.-J. Chen and J. Atai, Opt. Commun. **150**, 381 (1998).
[23] P. Muruganandam and S. K. Adhikari, Comput. Phys. Commun. **180**, 1888 (2009).